

Exchange mechanism of proton-proton scattering and the trend of polarized-beam cross sections at intermediate energies*

Francis Halzen† and Gerald H. Thomas
Argonne National Laboratory, Argonne, Illinois 60439
 (Received 24 January 1974)

We show how a few very general assumptions on the exchange mechanism in proton-proton scattering yield a simple description of the data recently obtained with the Argonne polarized beam. Predictions are presented for polarized cross sections in presently unexplored kinematic regions. We list the helicity amplitude decomposition of all possible observables in two tables.

Measurements with the polarized proton beam constructed at ANL will eventually lead to an amplitude analysis of proton-proton elastic scattering at intermediate energies. The data obtained so far^{1,2} have been taken on a target polarized transversely to the reaction plane. One will have to wait for experiments with the so-called *R* and *A* target polarizable in the beam direction, as well as in the direction orthogonal to the beam in the reaction plane, in order to achieve the separation of various amplitudes. We want to show in this note that the trend of the data obtained so far can be simply understood on the basis of very few general assumptions about the *t*-channel exchange mechanism. We show that

$$\frac{\sigma_{\uparrow\uparrow}}{\sigma} \approx 2 - \frac{\sigma_{\uparrow\uparrow}}{\sigma} \approx 1 + 2P, \tag{1}$$

$$\frac{\sigma_{\uparrow\uparrow}}{\sigma} = \frac{\sigma_{\uparrow\uparrow}}{\sigma} \approx 1, \tag{2}$$

$$\sigma_{\uparrow\uparrow}^{\text{tot}} \approx \sigma_{\uparrow\uparrow}^{\text{tot}}. \tag{3}$$

Throughout this paper σ_{ij} is a shorthand notation for the differential elastic cross section $d\sigma_{ij}/dt$, and σ_{ij}^{tot} denotes the *pp* total cross section; here *i* and *j* refer to the beam and target polarizations transverse to the reaction plane. In Eq. (1) *P* stands for the usual polarization parameter as measured with an unpolarized beam on a target polarized transversely to the reaction plane, and σ denotes the unpolarized differential cross section.

Equations (1) and (2) are in agreement with the present data^{1,2} as shown in Fig. 1. The right-hand side of Eq. (1) has been calculated using CERN polarization data³ and is shown as a shaded area. Also, Eq. (3) is verified at 3.5 GeV/*c*. Polarization data of Ref. 4 and Eq. (1) are explored to predict the intriguing behavior of polarized cross sections at lower energies, shown in Fig. 2.

In order to formulate the approximations in Eqs. (1)–(3), we introduce the standard *s*-channel helicity amplitudes⁵

$$\begin{aligned} \langle ++ | ++ \rangle &= H_1, \\ \langle -- | ++ \rangle &= H_2, \\ \langle + - | + - \rangle &= H_3, \\ \langle + - | - + \rangle &= H_4, \\ \langle ++ | + - \rangle &= H_5. \end{aligned} \tag{4}$$

H_1 , H_2 , and H_3 are net helicity-nonflip amplitudes; H_4 and H_5 are respectively double- and single-flip amplitudes. Combinations of the H_i have asymptotically definite quantum numbers in the *t* channel and are labeled as follows:

$$\begin{aligned} N_0 &= \frac{1}{2}(H_1 + H_3), \\ N_1 &= H_5, \\ N_2 &= \frac{1}{2}(H_4 - H_2), \\ A &= \frac{1}{2}(H_1 - H_3), \\ \pi &= \frac{1}{2}(H_4 + H_2). \end{aligned} \tag{5}$$

The amplitudes N_0 , N_1 , and N_2 are for natural-parity exchange, while A and π correspond to unnatural-parity exchange with A_1 and π, B quantum numbers, respectively.

The observables for a polarized beam scattered from a transversely polarized target can be expressed in terms of the amplitudes defined in Eq. (4):

$$\frac{\sigma_{\uparrow\uparrow}}{\sigma} = 1 + 2P + C_{nn}, \tag{6}$$

$$\frac{\sigma_{\uparrow\uparrow}}{\sigma} = 1 - 2P + C_{nn}, \tag{7}$$

$$\frac{\sigma_{\uparrow\uparrow}}{\sigma} = \frac{\sigma_{\uparrow\uparrow}}{\sigma} = 1 - C_{nn}, \tag{8}$$

with

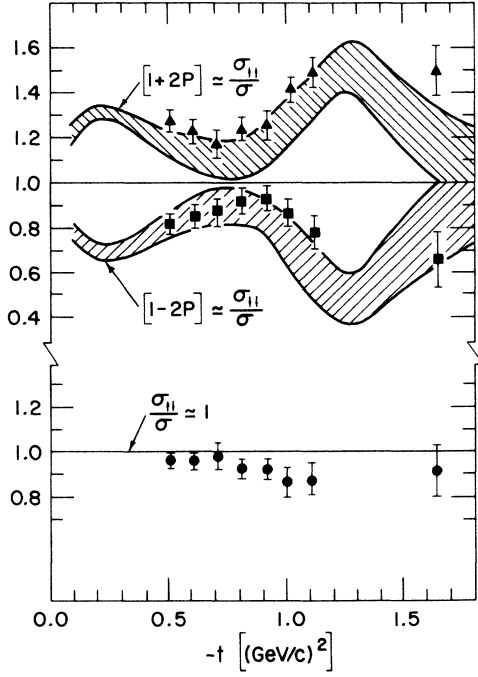


FIG. 1. Empirical tests of the relations (1) and (2),

$$\frac{\sigma_{\uparrow\uparrow}}{\sigma} = 1 + 2P,$$

$$\frac{\sigma_{\downarrow\downarrow}}{\sigma} = 1 - 2P,$$

$$\frac{\sigma_{\uparrow\downarrow}}{\sigma} = \frac{\sigma_{\downarrow\uparrow}}{\sigma} = 1,$$

at $p_{\text{lab}} = 6 \text{ GeV}/c$. σ_{ij} stands for polarized beam on polarized target differential cross sections, σ is the unpolarized differential cross section, and P is the conventional polarization parameter. The right-hand sides of the above relations are shown as a shaded area and evaluated with data from Ref. 3. Data for σ_{ij} are from Ref. 2.

$$\sigma = \frac{1}{2}(|H_1|^2 + |H_2|^2 + |H_3|^2 + |H_4|^2 + 4|H_5|^2), \quad (9)$$

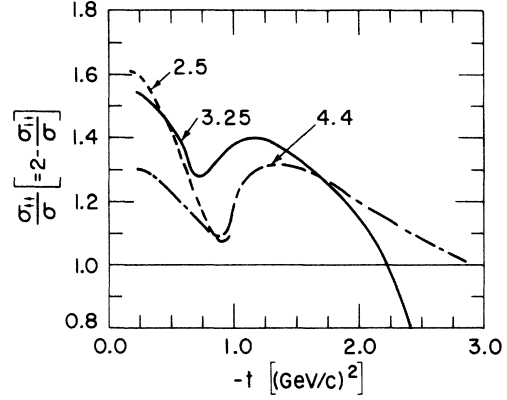
$$\sigma P = \text{Im}[(H_1 + H_2 + H_3 - H_4)H_5^*], \quad (10)$$

$$\sigma C_{nn} = \text{Re}(H_1 H_2^* - H_3 H_4^* + 2|H_5|^2). \quad (11)$$

It is obvious from Eqs. (6), (7), and (8) that the new information in the experiment is contained in the polarization parameter C_{nn} . It is very instructive to express C_{nn} in terms of the set of amplitudes (5):

$$\sigma C_{nn} = 2 \text{Re}(A\pi^* - N_0 N_2^* + |N_1|^2). \quad (12)$$

The first term in Eq. (12) is the product of two small unnatural-parity-exchange amplitudes. Our first assumption is that unnatural-parity exchange is small, and so this term is quadratically small. At 6 GeV/c this assumption is certainly safe. Our second assumption is that the remaining com-

FIG. 2. Relations (1) and (2) and data on the polarization parameter P from Ref. 4 are used to predict polarized differential cross sections at lower energies.

bination of natural-parity amplitudes is small. Two possible arguments in support of this are as follows:

(i) In a Regge-pole model for the natural-parity-exchange amplitudes, both the second and third terms in (12) are proportional to $(-t)$ and therefore kinematically suppressed (at least for small values of $|t|$).

(ii) If a single factorizable Regge pole dominates (say, the Pomeron), factorization implies the cancellation of the natural-parity contribution to C_{nn} as

$$\text{Re}(N_0 N_2^*) = |N_1|^2. \quad (13)$$

We therefore expect C_{nn} to be small at high energy, and consequently the polarization P determines all the observables in the experiment and Eqs. (6), (7), and (8) reduce to Eqs. (1) and (2).

Let us conclude with a brief discussion of our assumptions. π exchange is effectively measured in $n\bar{p}$ charge-exchange (CEX) reactions, and

$$\left(\frac{\sigma_{n\bar{p}}^{\text{CEX}}}{2\sigma_{p\bar{p}}} \right)^{1/2} \quad (14)$$

should represent a reliable estimate of the contribution of the π amplitude, relative to the leading natural-parity exchanges. Although (14) is small at 6 GeV/c, it grows to about 40% at 1 GeV/c. Thus, there is reason to believe C_{nn} could deviate substantially from zero at lower energies due to unnatural-parity-exchange contributions. [We ignore here the difficulty of estimating A in (12).] This has indeed been observed in an earlier low-energy experiment.⁶ We also remark that by the optical theorem, our assumptions yield Eq. (3) in agreement with 3.5-GeV/c data on total polarized cross sections.

In a picture where Pomeron, f , ω , ρ , and A_2 poles (or effective poles representing the effect of

TABLE I. The laboratory observables $I(\text{beam, target; scattered, recoil}) \equiv I(a, b; c, d)$ for $NN \rightarrow NN$ are defined with respect to a frame for each particle such that \hat{n} is along the normal to the scattering plane, \hat{l} is along the direction of motion, and $\hat{s} = \hat{n} \times \hat{l}$ is in the scattering plane. Since the target is at rest and \hat{l} is undefined, by convention we use for the target the beam unit vectors. θ_L and θ_R are the laboratory scattering and recoil angles, respectively. The observables $I(a, b; c, d)$ are just those measured with a polarized beam scattering off of a polarized target, with second scatterings performed to analyze the polarization of the scattered and recoil nucleon. In general, given the cross sections $\sigma(\pm, \pm, \pm, \pm)$ when each initial particle is polarized and each final particle's polarization analyzed parallel (+) or anti-parallel (-) to a given direction \hat{n} , \hat{l} , or \hat{s} , the ratio of the corresponding observable in the table to the unpolarized cross section is the ratio

$$\frac{\sum_{n_i} n_a n_b n_c n_d \sigma(n_a, n_b, n_c, n_d)}{\sum_{n_i} \sigma(n_a, n_b, n_c, n_d)},$$

where $n_i = \pm 1$. If an initial particle is unpolarized or a final particle's polarization is not analyzed, delete the corresponding factor n_i and omit the sums over this n_i . The vectors x , y , and z denote the center-of-mass helicity-frame directions. Their relationship to n , l , and s for each particle can be inferred from the table by noting that $I(a, b; c, d)$ is linear in its arguments: e.g., $I(\alpha s + \beta l, b; c, d) = \alpha I(s, b; c, d) + \beta I(l, b; c, d)$. The x , y , and z directions would be appropriate to polarization measurements in a colliding-beam measurement. The exchange amplitudes in the third part of the table are combinations of s -channel helicity amplitudes which asymptotically have definite t -channel quantum numbers. In terms of the usually defined amplitudes, $N_0 = \frac{1}{2}(\phi_1 + \phi_3)$, $N_1 = \phi_5$, $N_2 = \frac{1}{2}(\phi_4 - \phi_2)$, $\pi = \frac{1}{2}(\phi_4 + \phi_2)$, and $A = \frac{1}{2}(\phi_1 - \phi_3)$. In the text we use the other common notation H_i for ϕ_i .

Laboratory observables	Center-of-mass observables	Exchange amplitudes
$I(0, 0; 0, 0)$	$I(0, 0; 0, 0)$	$ N_0 ^2 + 2 N_1 ^2 + N_2 ^2 + \pi ^2 + A ^2$
$I(0, n; 0, 0)$	$-I(0, y; 0, 0)$	$-2 \text{Im}(N_0 - N_2)N_1^*$
$-I(0, l; 0, l) \cos \theta_R + I(0, l; 0, s) \sin \theta_R$	$I(0, z; 0, z)$	$ N_0 ^2 - N_2 ^2 - \pi ^2 + A ^2$
$I(0, l; 0, l) \sin \theta_R + I(0, l; 0, s) \cos \theta_R$	$I(0, z; 0, x)$	$-2 \text{Re}(N_0 + N_2)N_1^*$
$I(0, n; 0, n)$	$I(0, y; 0, y)$	$ N_0 ^2 + 2 N_1 ^2 + N_2 ^2 - \pi ^2 - A ^2$
$-I(0, s; 0, l) \sin \theta_R - I(0, s; 0, s) \cos \theta_R$	$I(0, x; 0, x)$	$ N_0 ^2 - N_2 ^2 + \pi ^2 - A ^2$
$I(l, l; 0, 0)$	$-I(z, z; 0, 0)$	$-2 \text{Re}(N_0 A^* - N_2 \pi^*)$
$I(s, l; 0, 0)$	$-I(x, z; 0, 0)$	$2 \text{Re}(\pi + A)N_1^*$
$I(n, n; 0, 0)$	$-I(y, y; 0, 0)$	$2 \text{Re}(A \pi^* - N_0 N_2^* + N_1 ^2)$
$I(s, s; 0, 0)$	$I(x, x; 0, 0)$	$2 \text{Re}(N_0 \pi^* - N_2 A^*)$
$I(n, 0; 0, n)$	$-I(y, 0; 0, y)$	$-2 \text{Re}(A \pi^* + N_0 N_2^* - N_1 ^2)$
$I(s, 0; 0, l) \sin \theta_R + I(s, 0; 0, s) \cos \theta_R$	$-I(x, 0; 0, x)$	$-2 \text{Re}(N_0 \pi^* + N_2 A^*)$
$-I(s, 0; 0, l) \cos \theta_R + I(s, 0; 0, s) \sin \theta_R$	$-I(x, 0; 0, z)$	$-2 \text{Re}(\pi - A)N_1^*$
$I(0, l; l, 0) \cos \theta_L + I(0, l; s, 0) \sin \theta_L$	$-I(0, z; z, 0)$	$-2 \text{Re}(N_0 A^* + N_2 \pi^*)$
$I(n, s; 0, l) \sin \theta_R + I(n, s; 0, s) \cos \theta_R$	$-I(y, x; 0, x)$	$2 \text{Im}(N_0 + N_2)N_1^*$
$I(s, n; 0, l) \sin \theta_R + I(s, n; 0, s) \cos \theta_R$	$I(x, y; 0, x)$	$2 \text{Im}(\pi - A)N_1^*$
$I(s, s; 0, n)$	$-I(x, x; 0, y)$	$-2 \text{Im}(\pi + A)N_1^*$
$I(n, s; 0, l) \cos \theta_R - I(n, s; 0, s) \sin \theta_R$	$I(y, x; 0, z)$	$2 \text{Im}(A \pi^* - N_0 N_2^*)$
$-I(s, n; 0, l) \cos \theta_R + I(s, n; 0, s) \sin \theta_R$	$I(x, y; 0, z)$	$2 \text{Im}(N_0 \pi^* + N_2 A^*)$
$I(l, n; 0, l) \sin \theta_R + I(l, n; 0, s) \cos \theta_R$	$I(z, y; 0, x)$	$2 \text{Im}(A N_0^* + \pi N_2^*)$
$I(l, s; 0, n)$	$-I(z, x; 0, y)$	$2 \text{Im}(A N_0^* - \pi N_2^*)$
$I(n, l; 0, l) \sin \theta_R + I(n, l; 0, s) \cos \theta_R$	$I(y, z; 0, x)$	$2 \text{Im}(A \pi^* + N_0 N_2^*)$
$I(s, l; 0, n)$	$I(x, z; 0, y)$	$-2 \text{Im}(N_0 \pi^* - N_2 A^*)$
$I(s, s; l, l) \sin \theta_L \sin \theta_R - I(s, s; s, s) \cos \theta_L \cos \theta_R$		
$+I(s, s; l, s) \sin \theta_L \cos \theta_R - I(s, s; s, l) \cos \theta_L \sin \theta_R$	$I(x, x; x, x)$	$ N_0 ^2 - 2 N_1 ^2 + N_2 ^2 + \pi ^2 + A ^2$
$-I(s, s; l, l) \sin \theta_L \cos \theta_R - I(s, s; s, s) \cos \theta_L \sin \theta_R$		
$+I(s, s; l, s) \sin \theta_L \sin \theta_R + I(s, s; s, l) \cos \theta_L \cos \theta_R$	$I(x, x; x, z)$	$2 \text{Re}(N_0 - N_2)N_1^*$
Optical theorem: $\sigma_{\text{tot}} = \frac{4\pi}{k} [I(0, 0) + P_s^{\text{beam}} P_s^{\text{target}} I(s, s) + P_n^{\text{beam}} P_n^{\text{target}} I(n, n) + P_l^{\text{beam}} P_l^{\text{target}} I(l, l)]$,		
$I(0, 0) = \text{Im}N_0$, $I(s, s) = I(n, n) = \text{Im}\frac{1}{2}(\pi - N_2)$, $I(l, l) = -\text{Im}A$		

cuts and nonleading singularities) dominate the natural-parity-exchange amplitudes, N_2 has to vanish as $-t$, as the double-flip amplitude H_4 also forces the nonflip amplitude H_2 to vanish like $-t$ in the combination

$$N_2 = \frac{1}{2}(H_4 - H_2).$$

This is, of course, related to the conspiracy problem. Both N_2 and $|N_1|^2$ are then kinematically suppressed at small $|-t|$, and relations (1) and (2) should become very reliable.

The previous argument makes it, however, difficult to understand the experimental suppression of C_{nn} at larger values of $|t|$. However, as pp scattering is exotic, duality implies an approximate cancellation of the secondary poles, leaving the Pomeron as the leading contribution. Its factorization would imply the cancellation of the natural-parity terms in Eq. (12) without necessarily requiring the polarization to vanish.

Only the experiments with the "R and A target" may ultimately sort out (a "road map" to the amplitudes is given in Tables I and II) whether the small nonzero values of C_{nn} observed at 6 GeV/c are due to unnatural-parity exchange or nonfactorizing cuts. Whatever the mechanism, we suggest the interesting possibility that C_{nn} remain small at lower energies, and hence we make the predictions of Fig. 2. Since by 1 GeV/c C_{nn} is known to be large, the rapid vanishing of C_{nn} as a function

TABLE II. Useful relations among observables, $(a, b; c, d) = \eta_a \eta_b \eta_c^* \eta_d^*(a', b'; c', d')$, in terms of center-of-mass helicity coordinates implicitly defined in Table I. See Thomas, Ref. 5. There are three more linear relations necessary in order to have a complete list:

$$I(x, x; z, z) = I(x, x; x, x) - I(y, y; 0, 0) - I(0, 0; 0, 0),$$

$$I(x, z; x, z) = I(x, x; x, x) + I(0, y; 0, y) - I(0, 0; 0, 0),$$

$$I(z, x; x, z) = -I(x, x; x, x) + I(y, 0; 0, y) + I(0, 0; 0, 0).$$

	η_0	η_x	η_y	η_z	$(a', b'; c', d')$
Parity	+	-	+	-	$(a, b; c, d)$
	+	-i	+	i	$(a, b; c, d) _{0 \leftrightarrow y; x \leftrightarrow z}$
Time reversal	+	-	+	+	$(c, d; a, b)$
Identical particles	+	-	-	+	$(b, a; d, c)$

of energy would be striking. We definitely expect our simple approach to be valid for energies above 6 GeV/c.

We thank A. D. Krisch and A. Yokosawa for making available data prior to publication. Discussions with V. Barger, R. Diebold, P. Hoyer, A. B. Wicklund, and A. Yokosawa are gratefully acknowledged. F. H. acknowledges the hospitality of the High Energy Physics Division at Argonne National Laboratory.

*Work supported by the U. S. Atomic Energy Commission.

†Permanent address: University of Wisconsin, Madison, Wisconsin 53706. Work supported in part by the University of Wisconsin Research Committee with funds granted by the Wisconsin Alumni Research Foundation, and in part by the U. S. Atomic Energy Commission under Contracts Nos. AT(11-1)-881, C00-881-399.

¹E. F. Parker *et al.*, Phys. Rev. Lett. **31**, 783 (1973).

²J. R. O'Fallon *et al.*, Phys. Rev. Lett. **32**, 77 (1974).

³M. Borghini *et al.*, Phys. Lett. **31B**, 405 (1970).

⁴A. Yokosawa (private communication); J. H. Parry *et al.*, Phys. Rev. D **8**, 45 (1973).

⁵See, e.g., C. Itzykson and M. Jacob, Nuovo Cimento **28**, 250 (1963); D. H. Sharp and W. G. Wagner, Phys. Rev. **131**, 2226 (1963); E. Leader and R. C. Slansky, *ibid.* **148**, 1491 (1966); R. J. N. Phillips, Nucl. Phys. **B2**, 394 (1967); G. H. Thomas, thesis, University of California (Los Angeles), 1969 (unpublished).

⁶A. Beretvas *et al.*, Rev. Mod. Phys. **39**, 536 (1967).